

Vision-Based Precision Approach and Landing for Advanced Air Mobility

*Evan Kawamura
Keerthana Kannan
Thomas Lombaerts
Corey Ippolito*

*NASA Ames Research Center (ARC): Intelligent Systems
Autonomous Systems – Perception & Distributed Sensing
2022 AIAA Scitech Forum
January 3, 2022*

This material is declared a work of the U.S. Government and is not subject to copyright protection in the United States.



Outline

1. Introduction
2. Kinematics & Dynamics
3. Tentative Vertiport Landing Light Configuration
4. Approach and Landing Profile
5. Extended Kalman Filter Design
6. Simulation Result
7. Conclusion



Problem

- AAM needs accurate and autonomous approach and landing systems
- Baseline perception and requirements come from existing technology: vision, IR, radar, glideslope indicators, GPS, etc.
- No active FAA vertiport documents for requirements (canceled in 2010 [1])
- Similar FAA document provides adequate requirements and standards: FAA AC 150/5390-2C: Heliport Design [2]
- FAA plays a critical role in enabling AAM operations, while NASA addresses technical and structural research gaps [3]

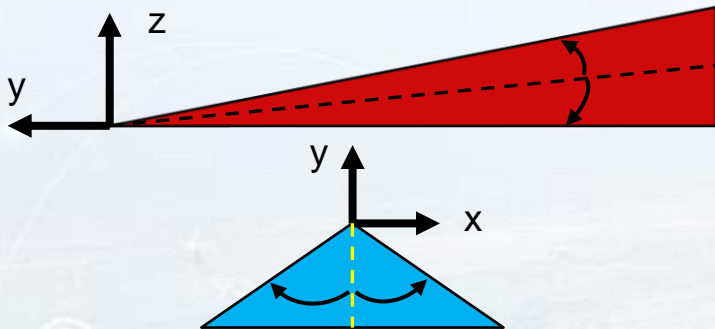
[1] Federal Aviation Administration, “AC 150/5390-3 (Cancelled) - Vertiport Design,” 2010. URL https://www.faa.gov/documentLibrary/media/advisory_circular/150-5390-3/150_5390_3.PDF

[2] Federal Aviation Administration, “AC 150/5390-2C - Heliport Design,” 2012. URL https://www.faa.gov/documentLibrary/media/Advisory_Circular/150_5390_2c.pdf

[3] National Academies of Sciences, Engineering, and Medicine, *Advancing Aerial Mobility: A National Blueprint*, The National Academies Press, 2020.



Instrument Landing System (ILS)

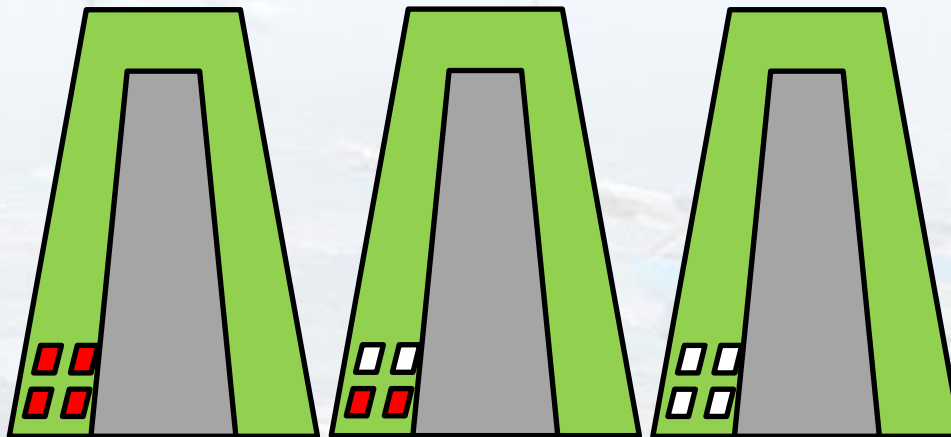


Glideslope: altitude deviation (**red**)
 Localizer: lateral deviation (**blue**)

Variations: Different Colors

Above glidepath
 On glidepath
 Below glidepath

Visual Approach Slope Indicator (VASI)

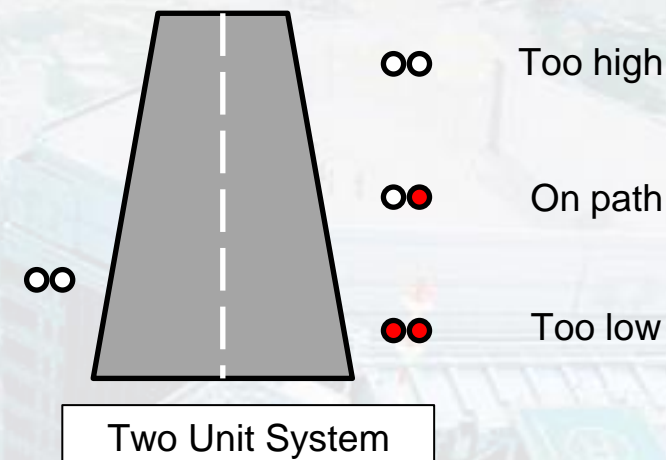
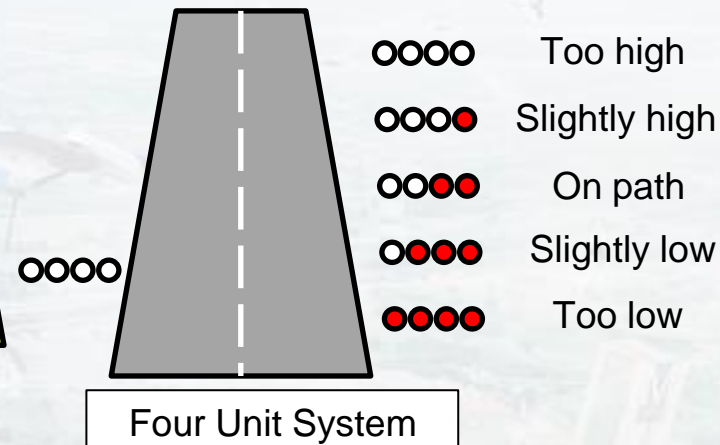


Far Bar:   
 Near Bar:   
 Below glidepath On glidepath Above glidepath

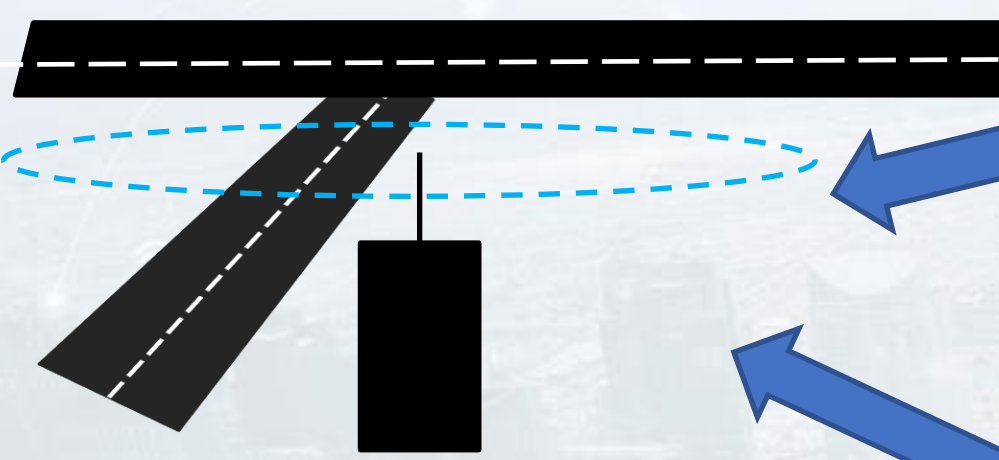
Variations: Pulsating Lights

Above glidepath: Pulsating white
 On glidepath: Steady white
 Slightly below glidepath: Pulsating red
 Below glidepath: Steady red

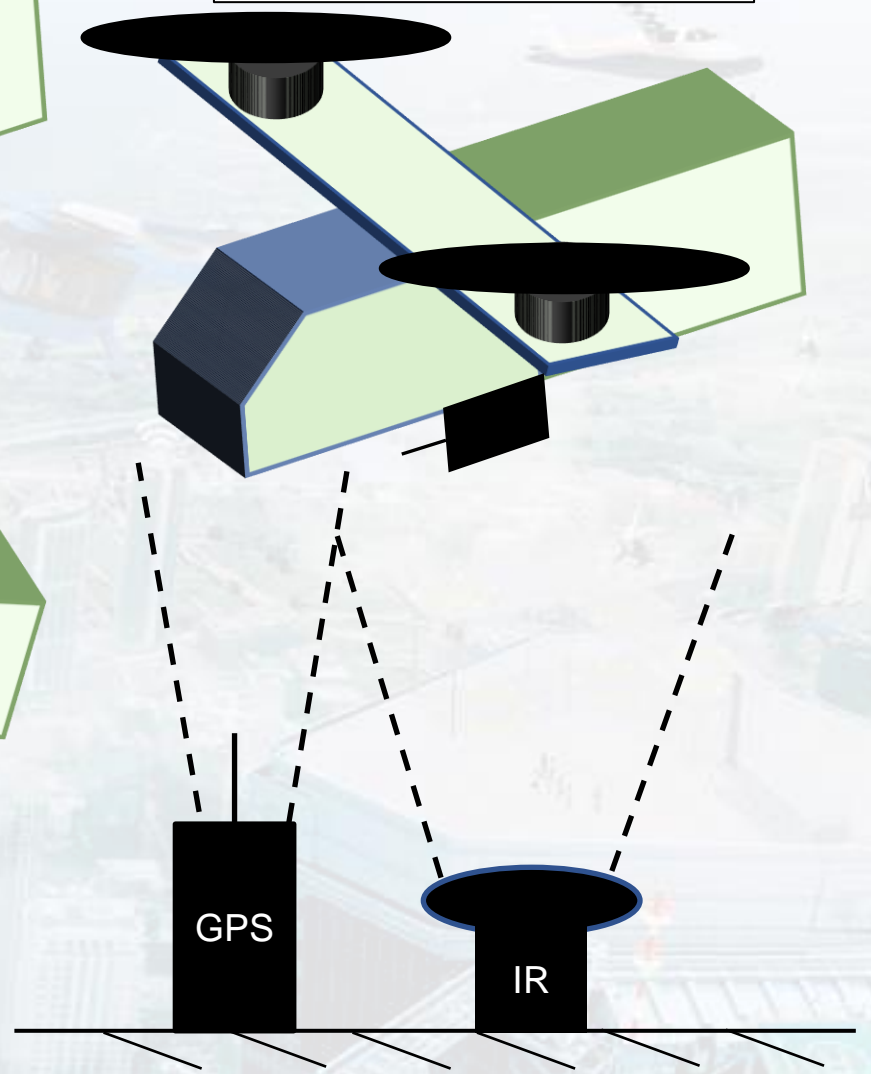
Precision Approach Path Indicator (PAPI)



Ground Based Augmentation System (GBAS)



GPS & IR Beacons



- Has more flexibility and economic benefits than ILS
- Several approach angles for landing
- Transitioning from ILS to GBAS will potentially take decades

[4] Wang, Z., Wang, S., Zhu, Y., and Xin, P., "Assessment of ionospheric gradient impacts on ground-based augmentation system (GBAS) data in Guangdong province, China," *Sensors*, Vol. 17, No. 10, 2017, p. 2313.



Coplanar POSIT Algorithm

- POSIT = **P**ose from **O**rthography and **S**caling with **I**terations
- Goal: compute rotation and translation of the object

http://www.daniel.umiacs.io/Site_2/Code.html

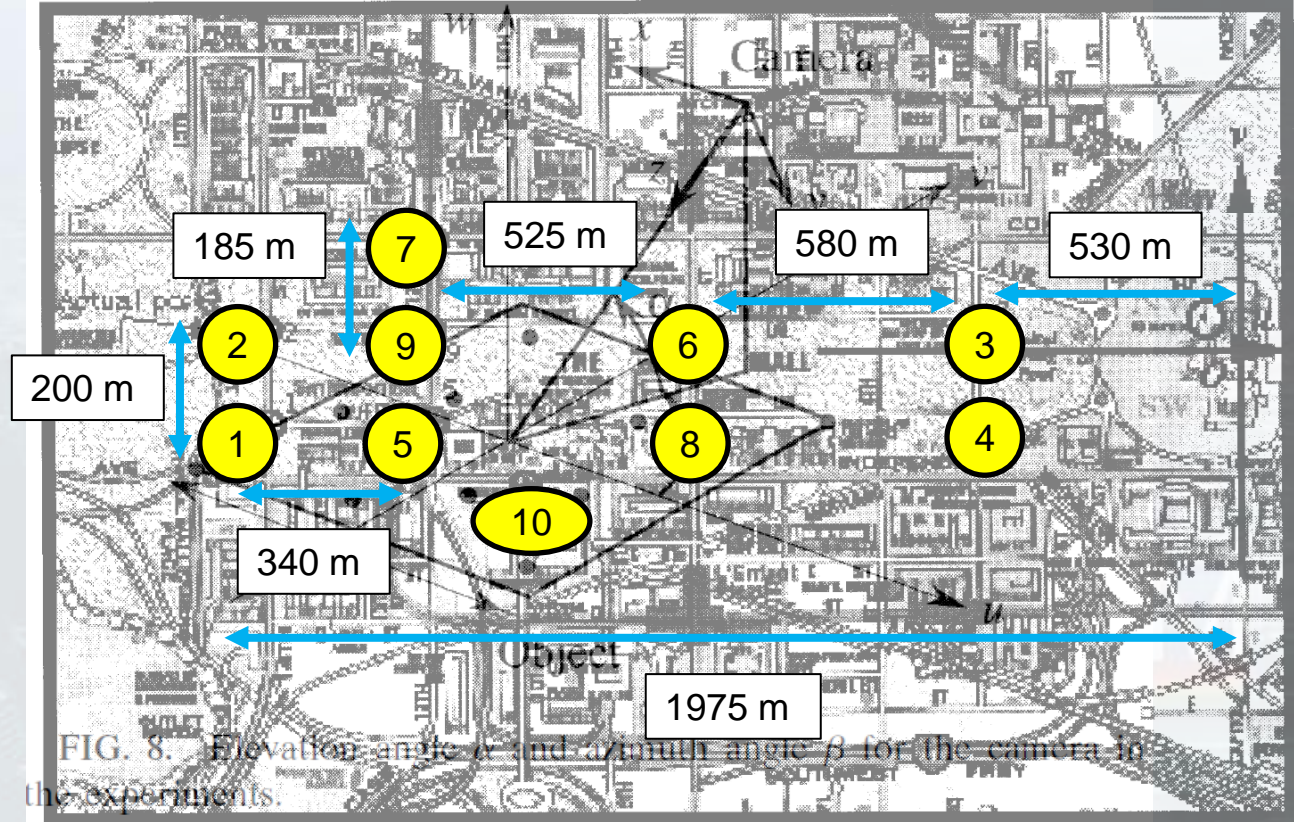


FIG. 14. Topographic map of the area, with feature points and object coordinate system.

Constraint: requires at least four coplanar points

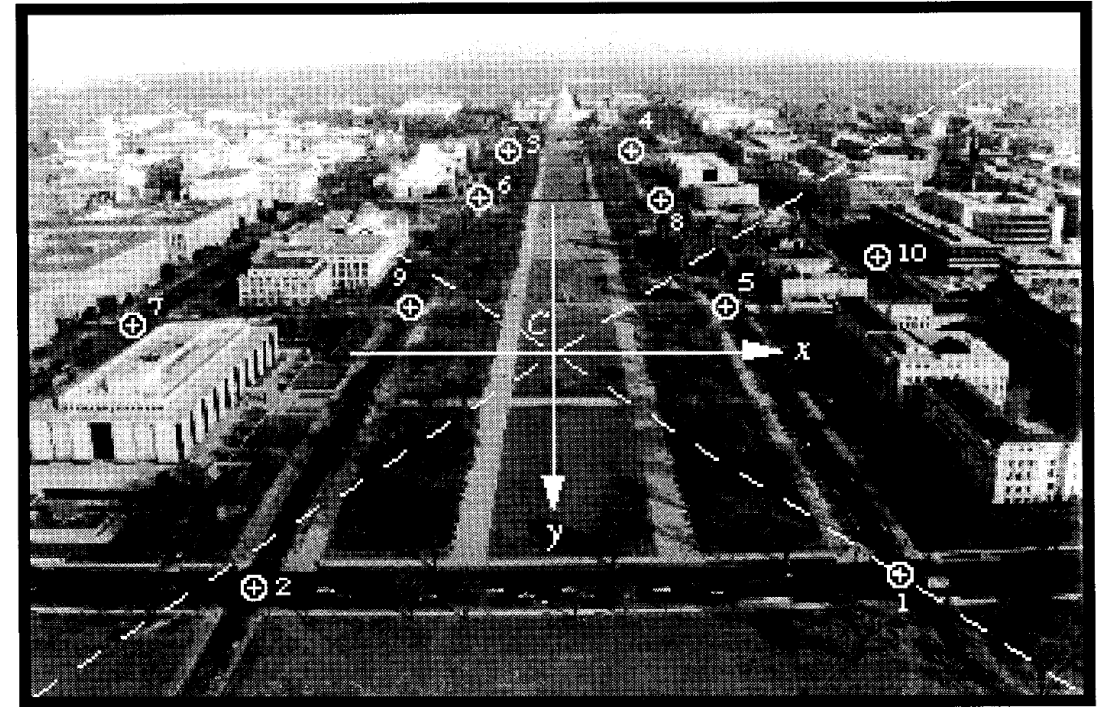


FIG. 13. The Mall in Washington, D.C., from the top of the Washington Monument, with feature points and image coordinate system.

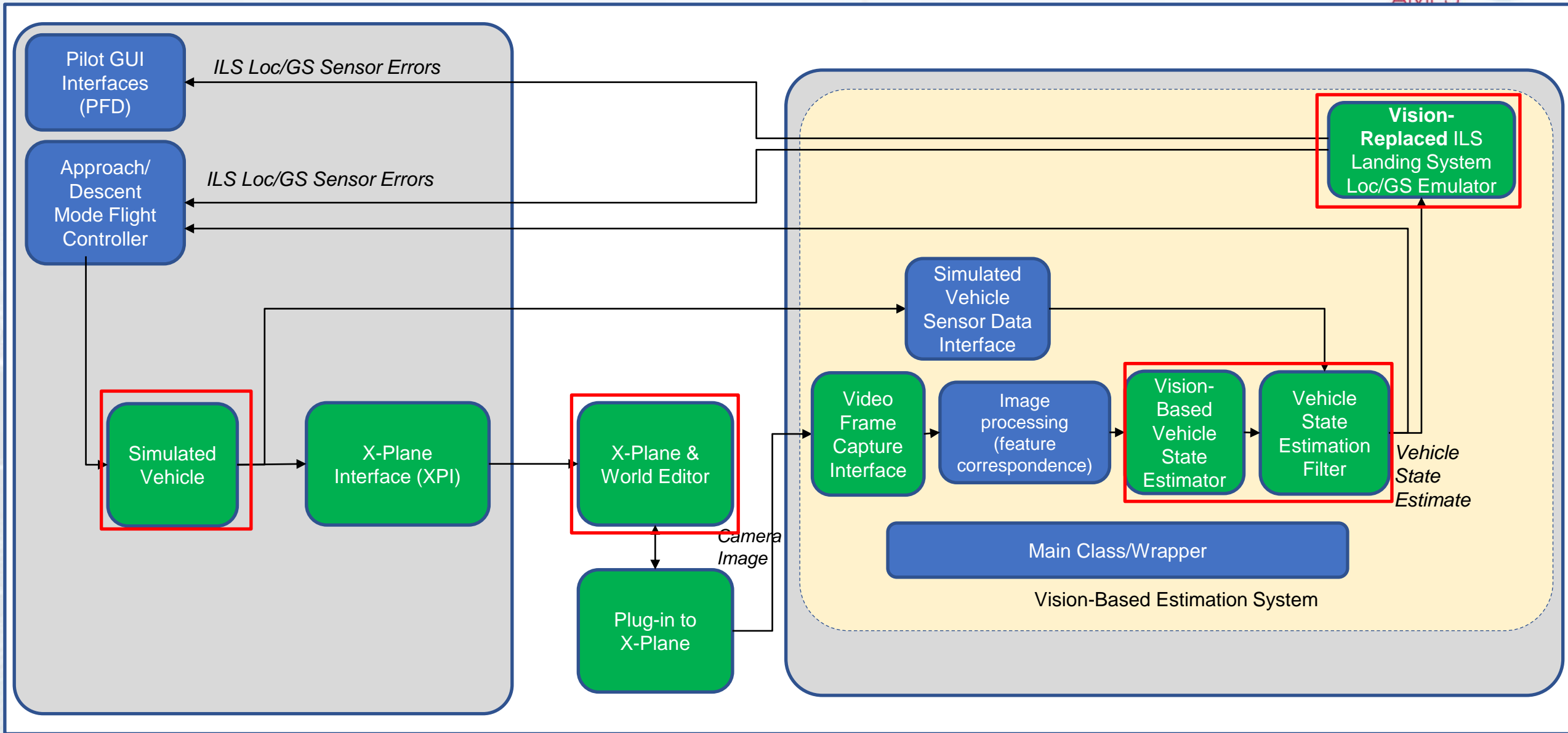
Experiment at Mall in Washington, DC
 (camera at the top of Washington Monument):
 $\Delta U = 3\text{ m}, \Delta V = 4\text{ m}, \Delta W = 2\text{ m}$

Overview of Work

- Use FAA AC 150/5390-2C: Heliport Design for baseline requirements and standards
- Implement coplanar POSIT for vision-based AAM navigation
- Deliver perception precision approach and landing requirements and data sets to other NASA projects and industry partners
- Provides AAM safe and accurate approach and landing
- Autonomous approach and landing removes pilots -> increase efficiency and payload capacity
- Paves the way for AAM approach and landing research to enhance future AAM operations



Overview of Work



Outline

1. Introduction
2. Kinematics & Dynamics
3. Tentative Vertiport Landing Light Configuration
4. Approach and Landing Profile
5. Extended Kalman Filter Design
6. Simulation Results
7. Conclusion



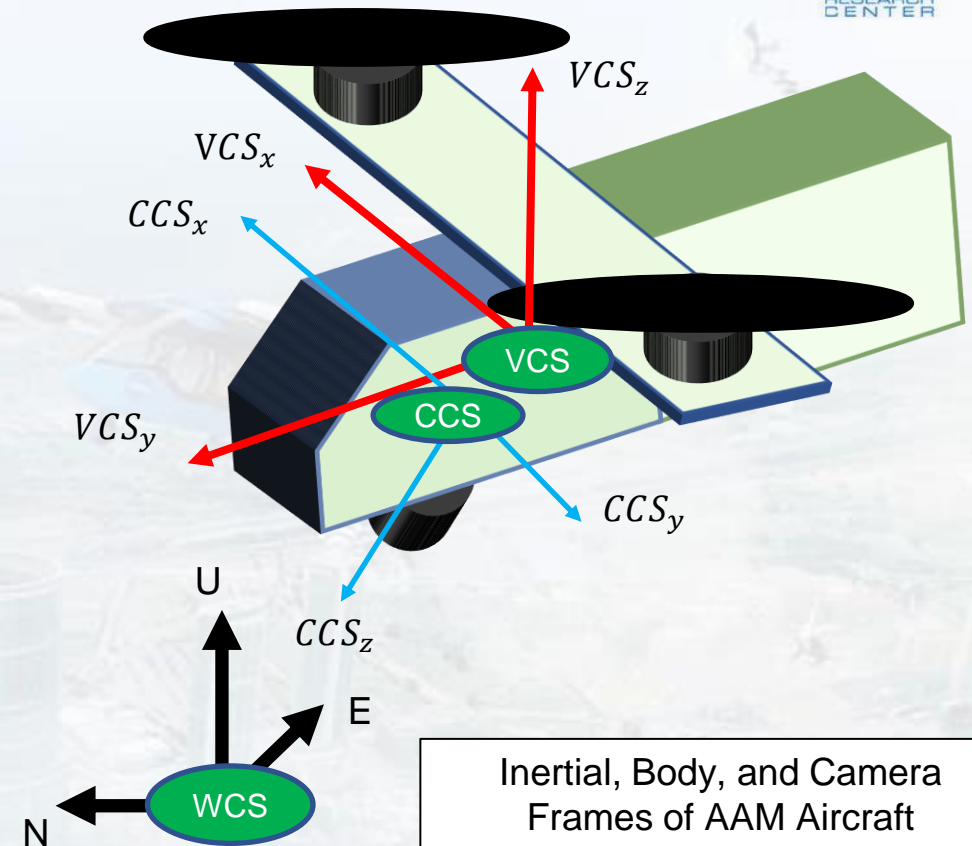
- State vector:
 - $s = [N \ E \ U \ v_N \ v_E \ v_U \ \phi \ \theta \ \psi]^T$
- Direction cosine matrix (3-1-2)
- Relation between body angular velocity and Euler angular rates [6]:

$$\Omega = \begin{bmatrix} 0 & \cos \phi & -\cos \theta \sin \phi \\ 1 & 0 & \sin \theta \\ 0 & \sin \phi & \cos \theta \cos \phi \end{bmatrix} \dot{\Theta}$$

$$\Omega = [r \ q \ p]^T, \dot{\Theta} = [\dot{\psi} \ \dot{\theta} \ \dot{\phi}]^T$$

- Relate body frame velocities to inertial velocities through DCM [6]:

$$\begin{bmatrix} v_N \\ v_E \\ v_U \end{bmatrix} = \begin{bmatrix} -s\psi s\theta s\phi + c\phi c\psi & -c\theta s\psi & c\phi s\theta s\psi + s\phi c\psi \\ s\phi s\theta c\psi + c\phi s\psi & c\theta c\psi & -c\phi s\theta c\psi + s\phi s\psi \\ -s\phi c\theta & s\theta & c\phi c\theta \end{bmatrix} \begin{bmatrix} u \\ v \\ w \end{bmatrix}$$



Inertial, Body, and Camera Frames of AAM Aircraft

WCS = World Coordinate System (inertial)
VCS = Vehicle Coordinate System (body)
CCS = Camera Coordinate System

[6] Schaub, H., and Junkins, J. L., Analytical Mechanics of Space Systems, 4th ed., AIAA, 2018.

- General aircraft translational dynamic equations:

- $F_x = m(\dot{u} + qw - rv) + mg \sin \theta$
- $F_y = m(\dot{v} + ru - pw) - mg \cos \theta \sin \phi$
- $F_z = m(\dot{w} + pv - qu) - mg \cos \theta \cos \phi$

Take accelerometer measurements assuming at CG
→ specific aerodynamic forces

- Specific forces (accelerometers)

- $F_x = A_x m, F_y = A_y m, F_z = A_z m$

- General kinematic equations for all aircraft:

- $\dot{u} = A_x - g \sin \theta - qw + rv$
- $\dot{v} = A_y - g \cos \theta \sin \phi - ru + pw$
- $\dot{w} = A_z + g \cos \theta \cos \phi - pv + qu$

1. Combine general aircraft translational dynamic equations with accelerometer measurements at CG
2. Divide by mass

[7] Chu, P., Mulder, J. A. B., and Breeman, J., "Real-time identification of aircraft physical models for fault tolerant flight control," *Fault Tolerant Flight Control*, Springer, 2010, pp. 129–155.



Outline

1. Introduction
2. Kinematics & Dynamics
3. Tentative Vertiport Landing Light Configuration
4. Approach and Landing Profile
5. Extended Kalman Filter Design
6. Simulation Results
7. Conclusion



Tentative Vertiport Landing Light Configuration

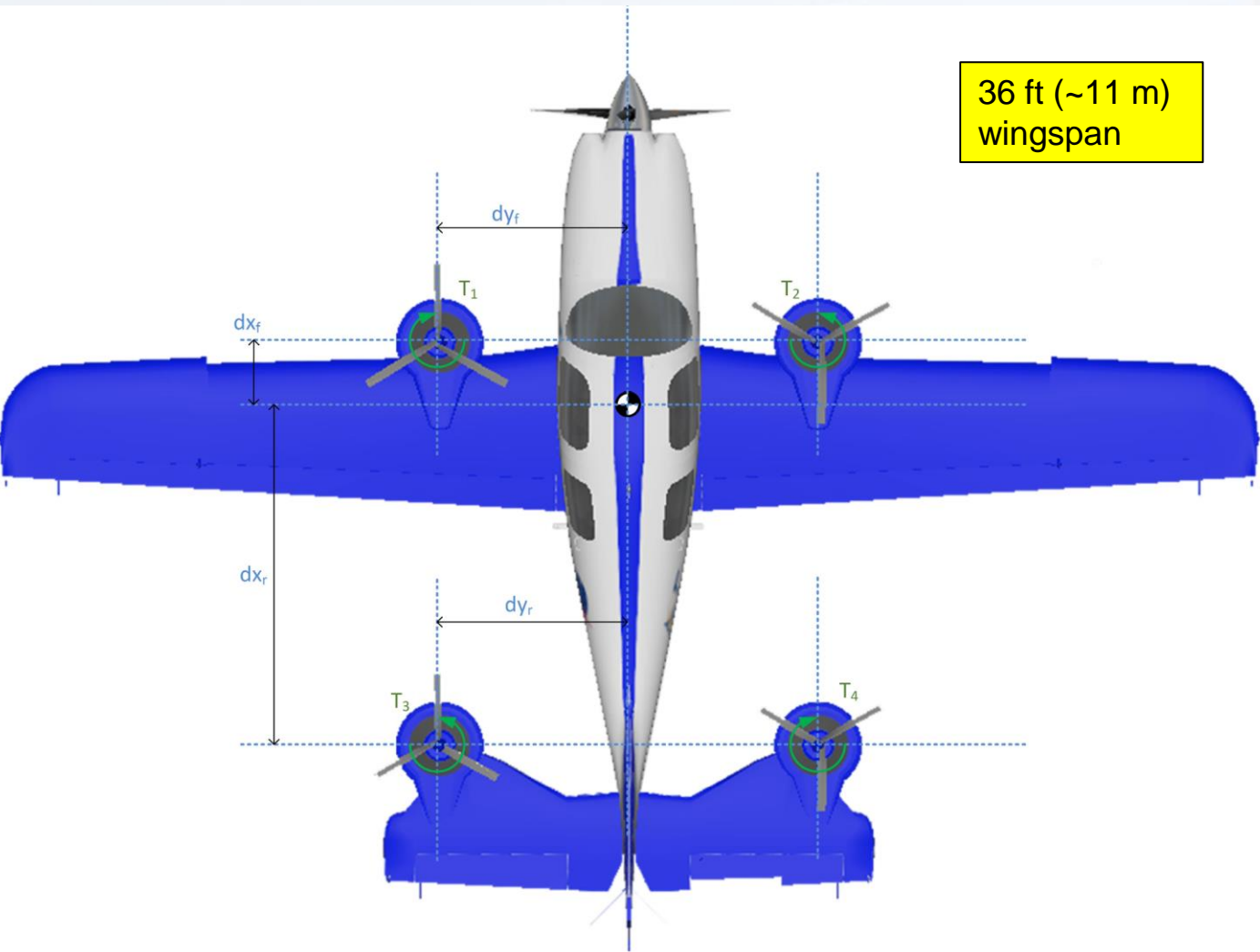


Fig. 2 Geometry of the UAM concept model

[8] Lombaerts, T., Kaneshige, J., Schuet, S., Aponso, B. L., Shish, K. H., and Hardy, G., "Dynamic Inversion based Full Envelope Flight Control for an eVTOL Vehicle using a Unified Framework," AIAA Scitech 2020 Forum, 2020, p. 1619.

Fig. 2-2 of FAA AC: 150/5390-2C – Heliport Design [2]

RD -> Wingspan

TLOF = Touchdown & Liftoff area

FATO = Final Approach and Take Off

TLOF: $11 \times 11 \text{ m}^2$

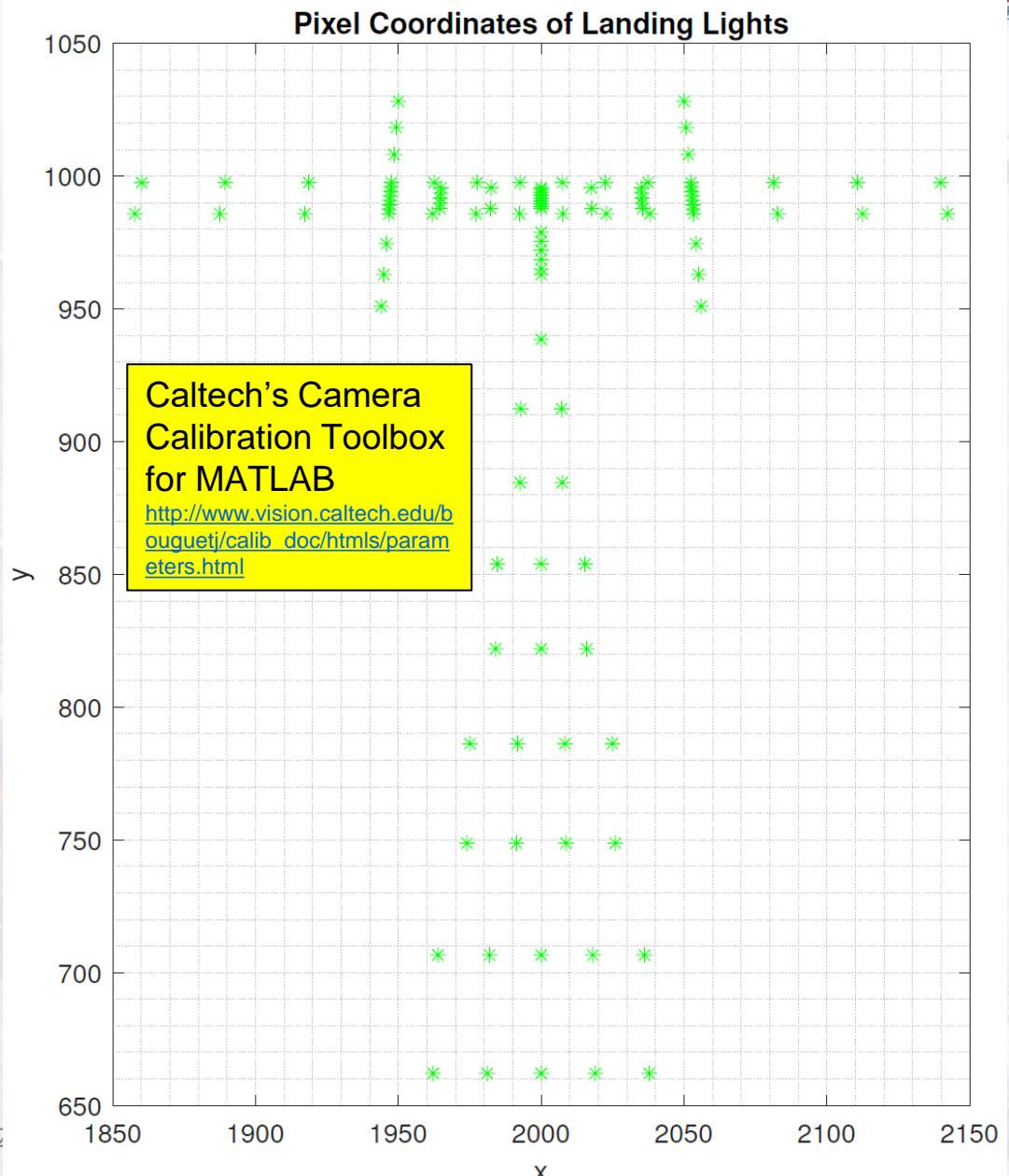
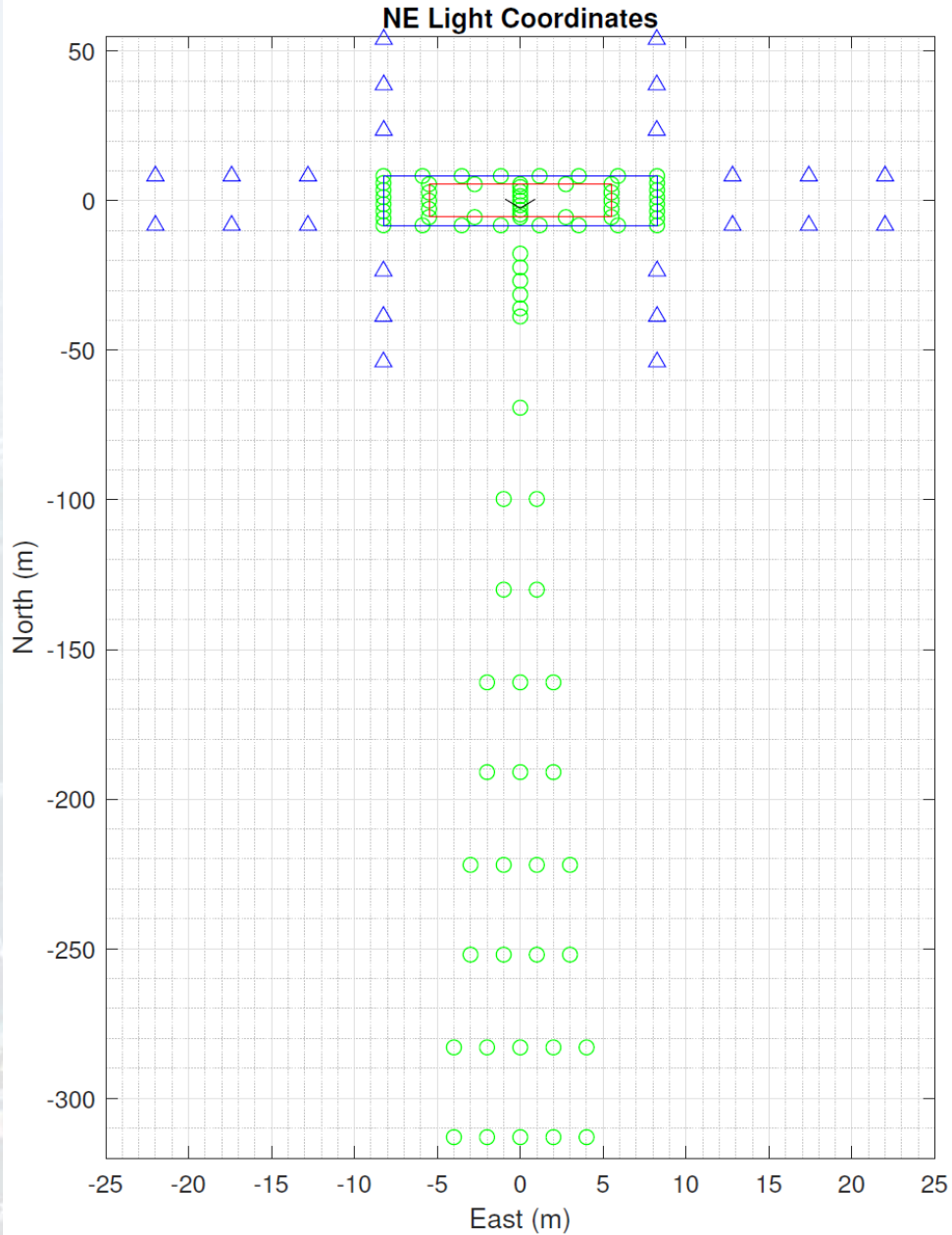
FATO: $16.5 \times 16.5 \text{ m}^2$

DIM	ITEM	VALUE	NOTES
A	Minimum TLOF Length	1 RD	
B	Minimum TLOF Width	1 RD	
C	Minimum FATO Length	$1 \frac{1}{2} D$	See Paragraph 207.a.(1) and Figure 2-5 for adjustments of elevations above 1000'
E	Minimum FATO Width	$1 \frac{1}{2} D$	
F	Minimum Separation Between the Perimeters of the TLOF and FATO	$\frac{3}{4} D - \frac{1}{2} RD$	
G	Minimum Safety Area Width	See Table 2-1	

Note: For a circular TLOF and FATO, dimensions A, B, C and E refer to diameters.

Figure 2-2. TLOF/FATO Safety Area Relationships and Minimum Dimensions: General Aviation

Tentative Vertiport Landing Light Configuration

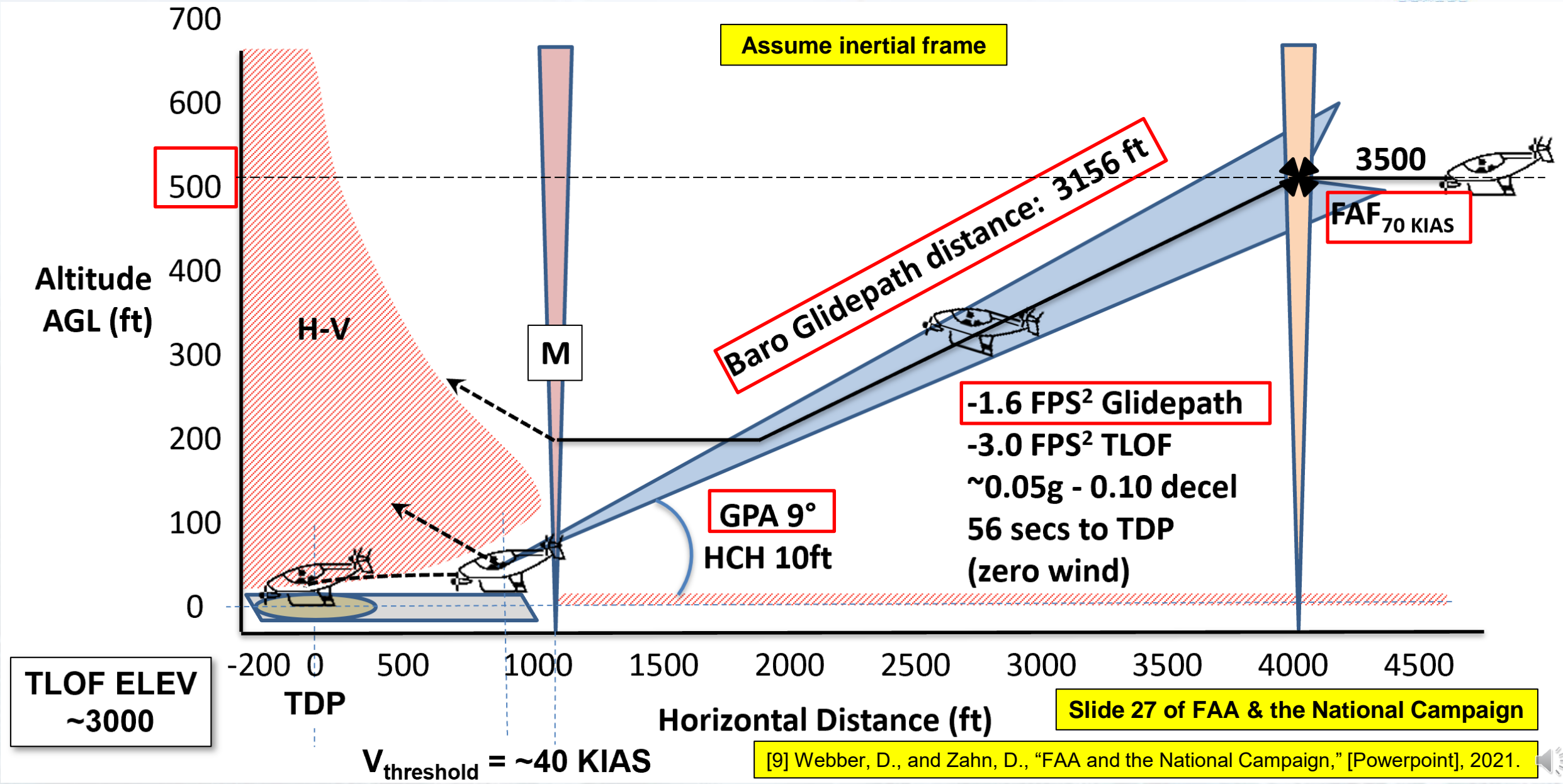


Outline

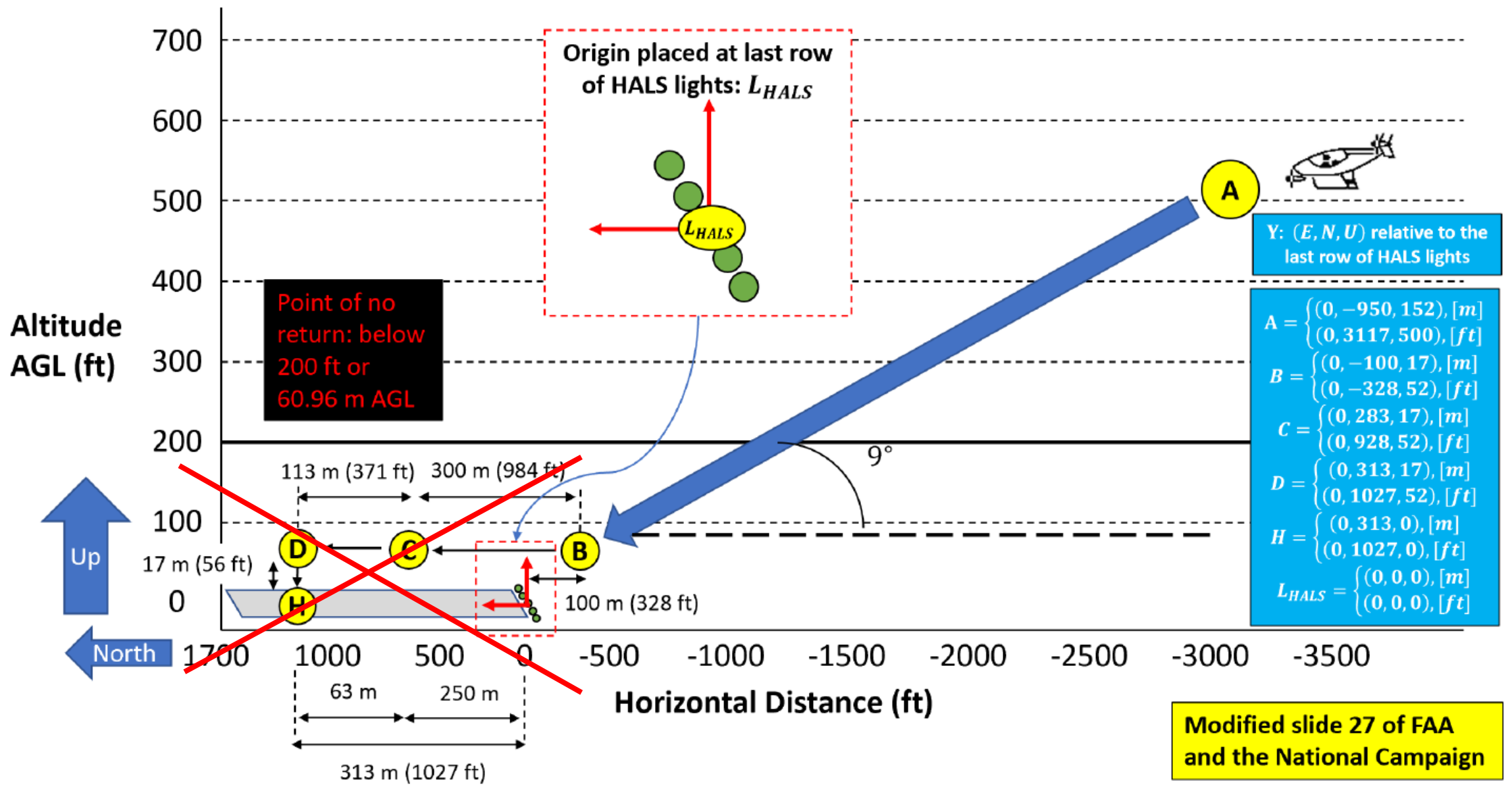
1. Introduction
2. Kinematics & Dynamics
3. Tentative Vertiport Landing Light Configuration
4. Approach and Landing Profile
5. Extended Kalman Filter Design
6. Simulation Results
7. Conclusion



Approach and Landing Profile



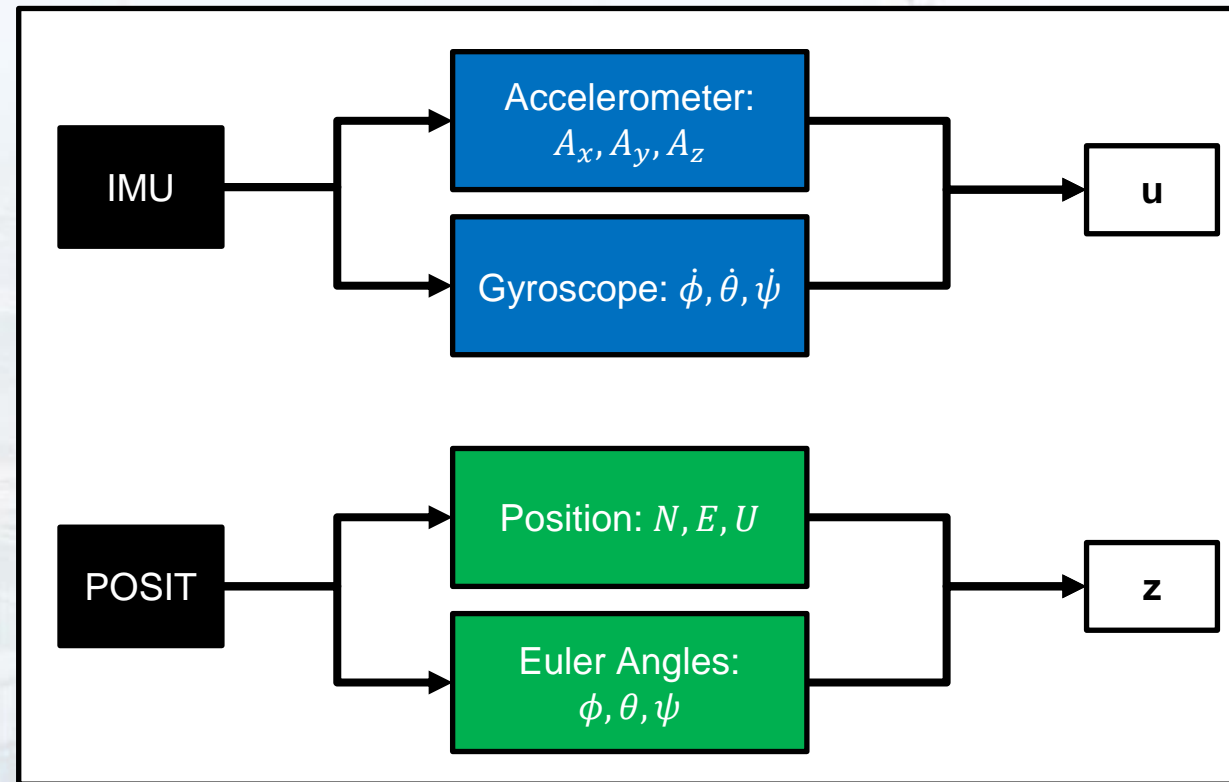
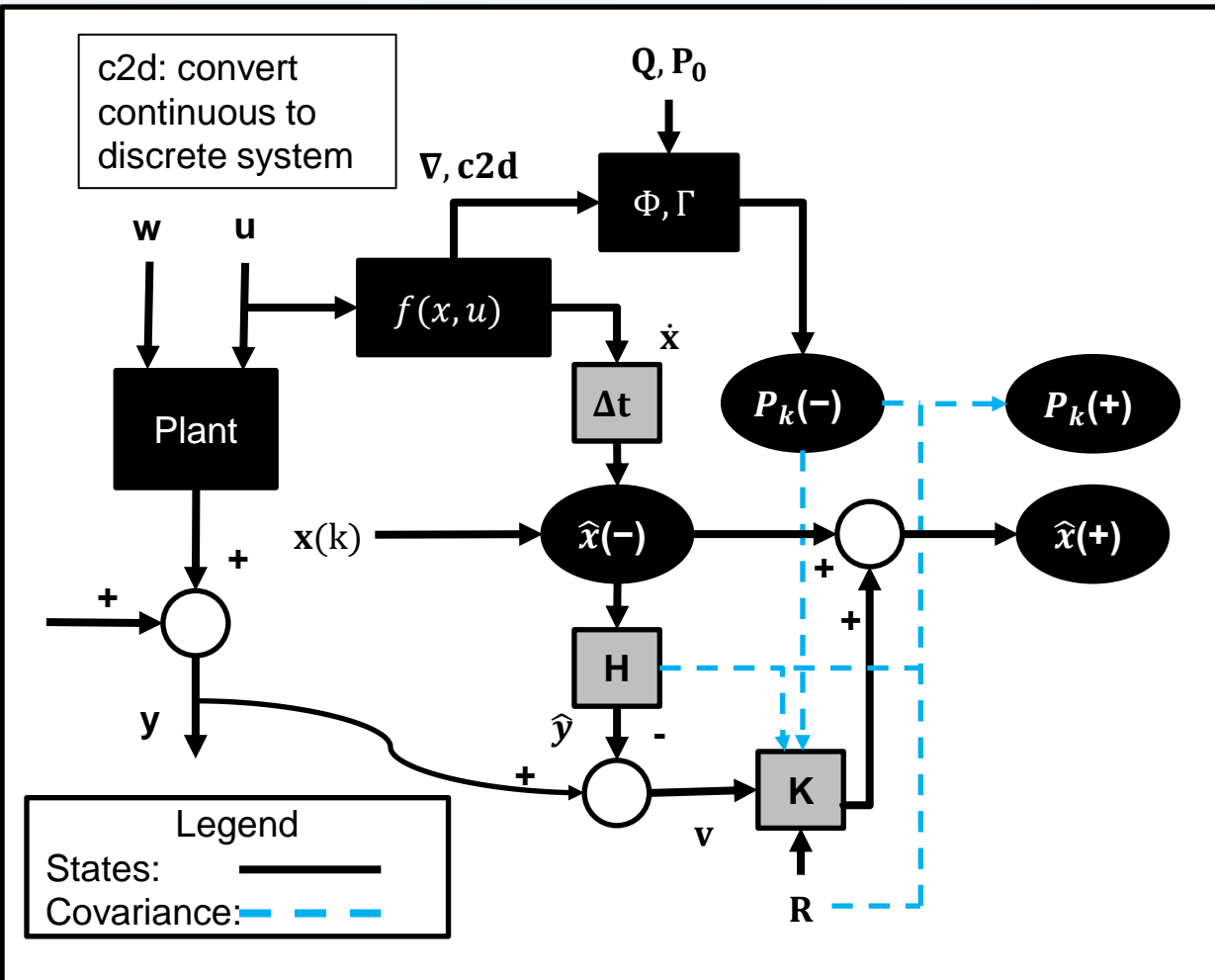
Approach and Landing Profile



Outline

1. Introduction
2. Kinematics & Dynamics
3. Tentative Vertiport Landing Light Configuration
4. Approach and Landing Profile
5. Extended Kalman Filter Design
6. Simulation Results
7. Conclusion





[10] Stepanyan, V., Lombaerts, T., Shish, K. H., and Cramer, N. B., "Adaptive Multi-Sensor Information Fusion For Autonomous Urban Air Mobility Operations," AIAA Scitech 2021 Forum, 2021, p. 1115.
 [11] Gelb, A., Applied Optimal Estimation, MIT press, 1974.
 [12] Simon, D., Optimal State Estimation: Kalman, H1, and Nonlinear Approaches, John Wiley & Sons, 2006.

Outline

1. Introduction
2. Kinematics & Dynamics
3. Tentative Vertiport Landing Light Configuration
4. Approach and Landing Profile
5. Extended Kalman Filter Design
6. Simulation Results
7. Conclusion



- East estimation is the most accurate
- North estimation is the least accurate

$$\Delta p = \sqrt{\Delta N^2 + \Delta E^2 + \Delta U^2}$$

E_{des}	N_{des}	U_{des}	E_{est}	N_{est}	U_{est}	ΔE	ΔN	ΔU	Δp
0	-950	152	0	-948.2	151.84	0	1.794	-0.1564	1.801
0	-850	136	0	-845.9	135.63	0	4.071	-0.3699	4.087
0	-750	120	-0.1434	-745.1	119.46	-0.1434	4.942	-0.5428	4.974
0	-650	104	0.1241	-644.9	103.53	0.1241	5.062	-0.4698	5.086
0	-550	88	0	-548.0	88.07	0	2.026	0.07176	2.027
0	-450	72	-0.0867	-450.4	72.40	-0.08668	-0.4449	0.3966	0.602
0	-350	56	0	-347.9	55.91	0	2.119	-0.0877	2.121
0	-250	40	-0.04761	-247.4	39.95	-0.04761	2.636	-0.0501	2.637
0	-150	24	0	-148.0	23.99	0	1.983	-0.008429	1.983
0	-100	16	-0.01888	-98.1	16.01	-0.01888	1.934	0.00991	1.935



$$\phi_{des} = 0^\circ \quad \theta_{des} = -9^\circ \quad \psi_{des} = 0^\circ$$

$$\Delta\Theta = \sqrt{\Delta\phi^2 + \Delta\theta^2 + \Delta\psi^2}$$

E_{des}	N_{des}	U_{des}	ϕ_{est}	θ_{est}	ψ_{est}	$\Delta\phi$	$\Delta\theta$	$\Delta\psi$	$\Delta\Theta$
0	-950	152	0.2421	-8.969	-0.2394	-0.2421	-0.03142	0.2394	0.3419
0	-850	136	0.1721	-8.975	-0.1696	-0.1721	-0.02539	0.1696	0.2430
0	-750	120	0.1060	-8.968	-0.1001	-0.1060	-0.03177	0.1001	0.1492
0	-650	104	-0.1605	-8.974	0.1543	0.1605	-0.02584	-0.1543	0.2241
0	-550	88	-0.1087	-9.014	0.1079	0.1087	0.01351	-0.1079	0.1537
0	-450	72	0.0653	-9.031	-0.06225	-0.06534	0.03135	0.06225	0.09554
0	-350	56	-0.0400	-8.986	0.03924	0.03999	-0.01378	-0.03924	0.05770
0	-250	40	-0.0392	-9.000	0.03974	0.03918	-0.000318	-0.03974	0.05580
0	-150	24	-0.0872	-8.995	0.08633	0.08719	-0.00453	-0.08633	0.1228
0	-100	16	-0.00245	-9.002	0.00308	0.00245	0.00195	-0.00308	0.00439



Simulation Results: VMS Telemetry Data



- VMS at NASA Ames Research Center
- Modified Vertical Motion Simulator (VMS) telemetry data for a 9° glideslope (manual control)
- Extract IMU data: accelerometer & gyroscope in body frame → u (EKF)



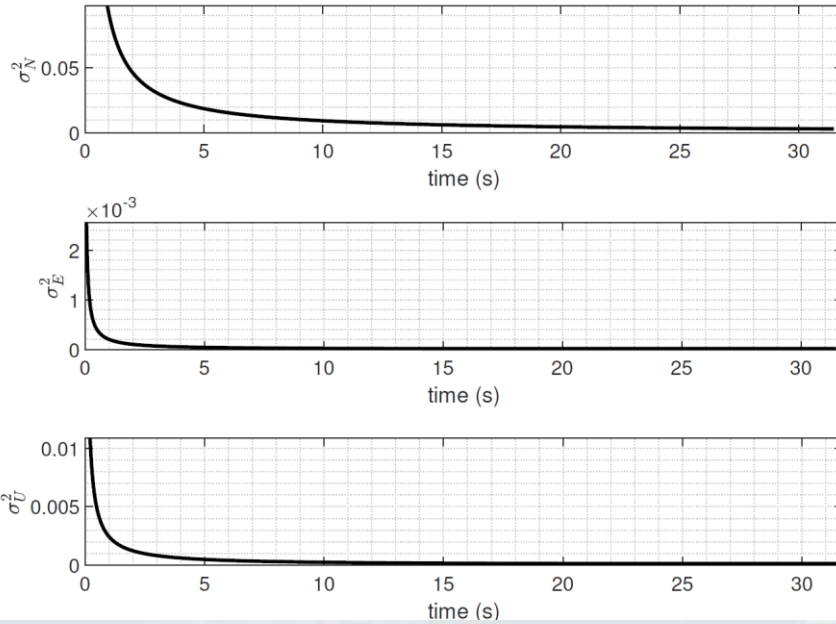
Original Trajectory (Google Earth)



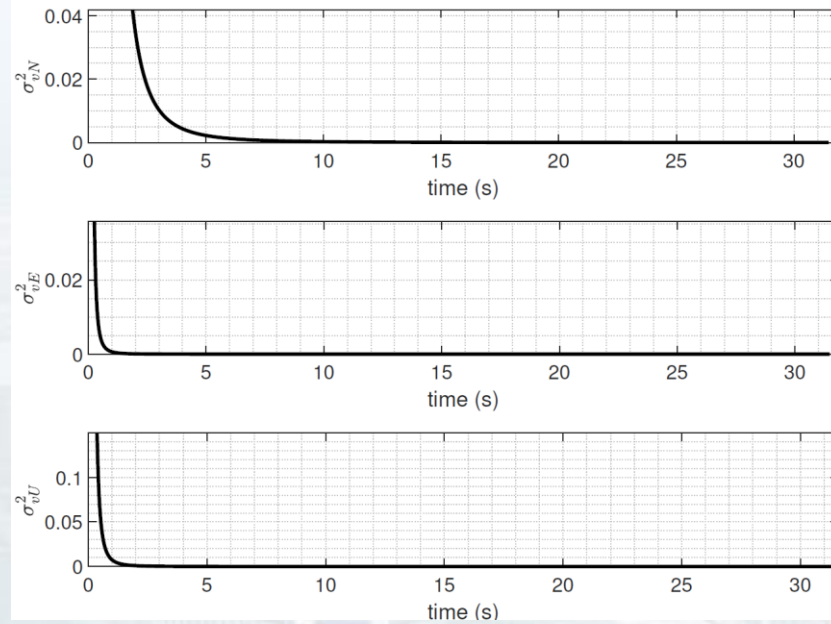
VMS cockpit display



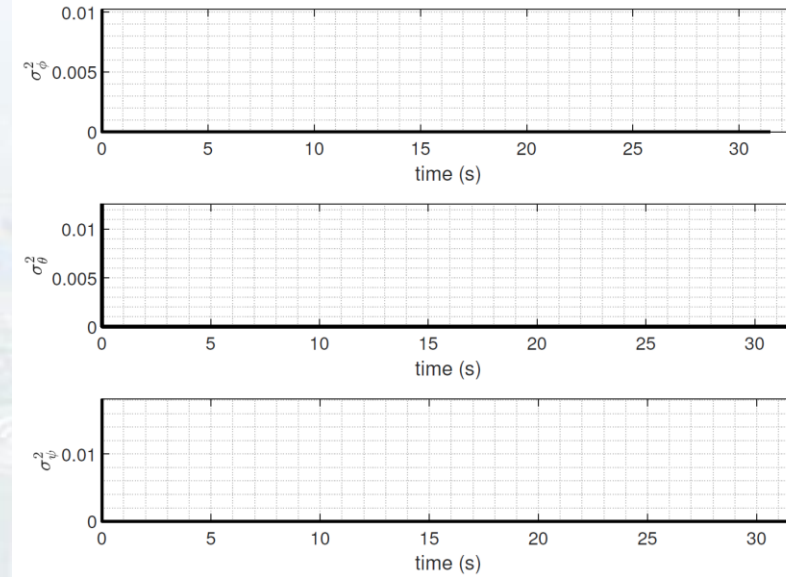
Error Covariance for Position



Error Covariance for Velocity



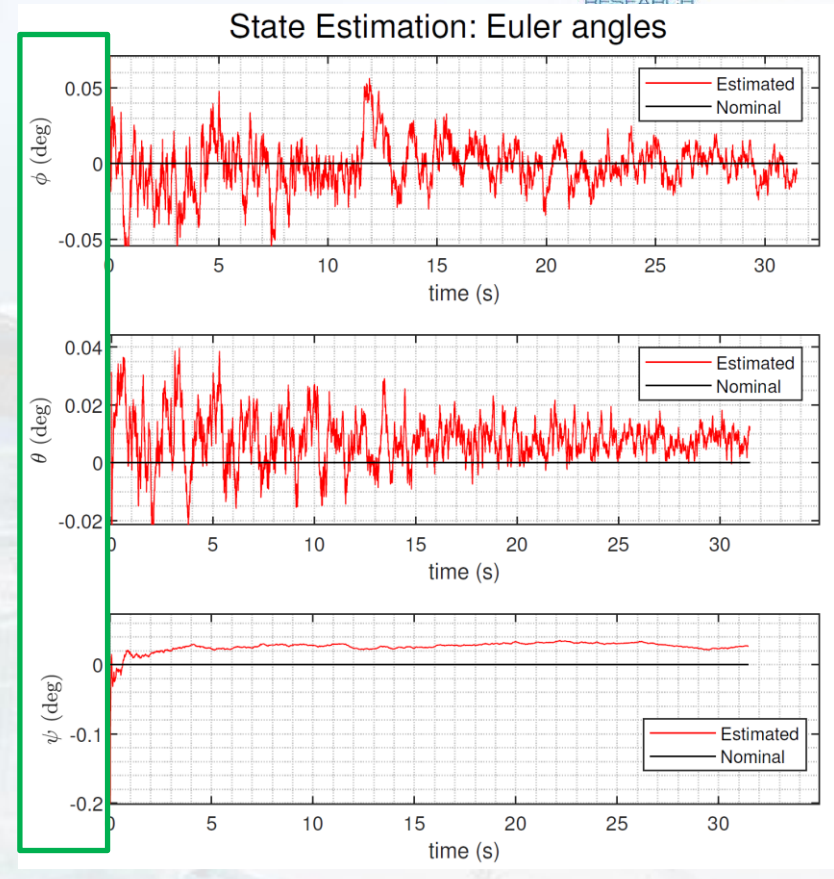
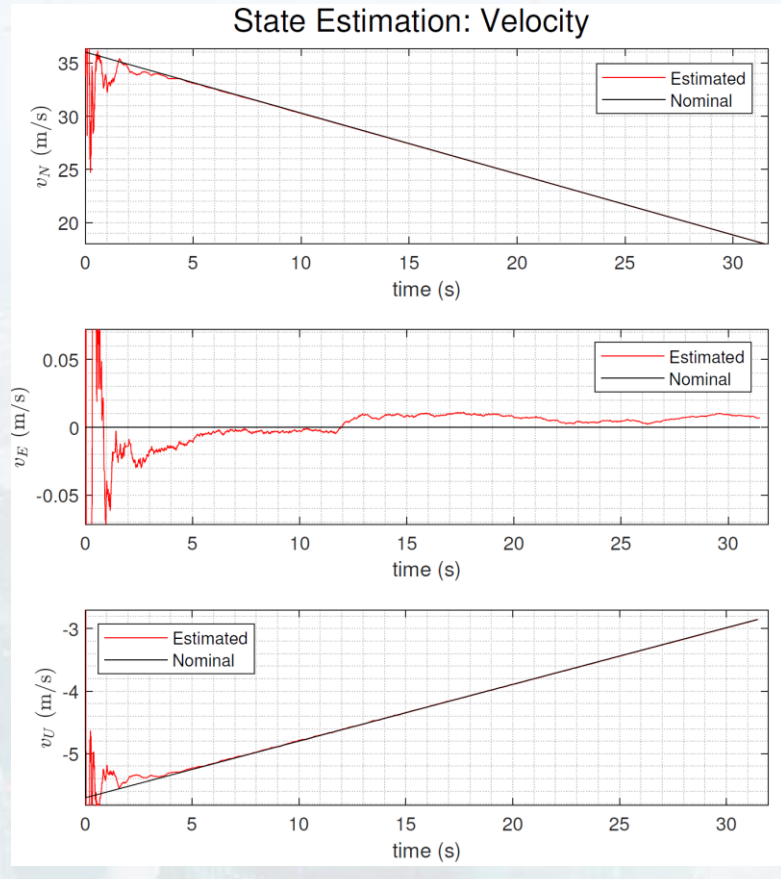
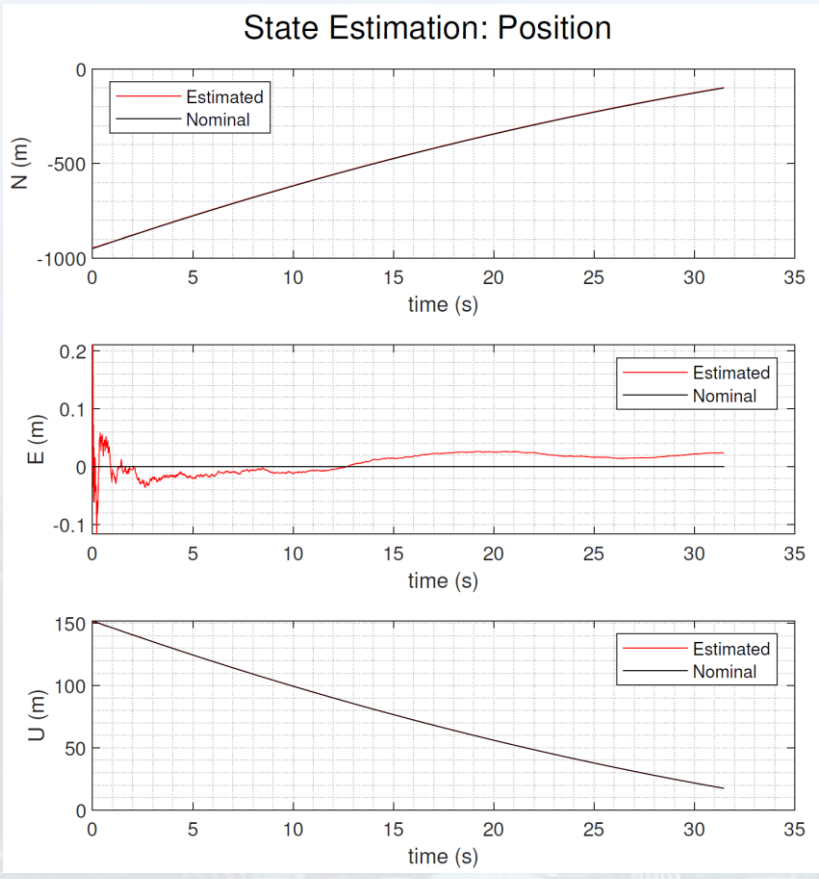
Error Covariance for Euler angles



- Quick convergence
- Initial covariance values were 1000
- High confidence (low uncertainty) in state estimation
- Runtime of 2 ms per iteration -> real-time capabilities and onboard implementation in the future



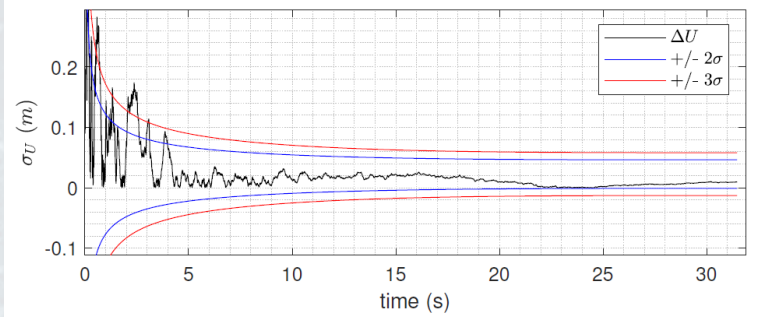
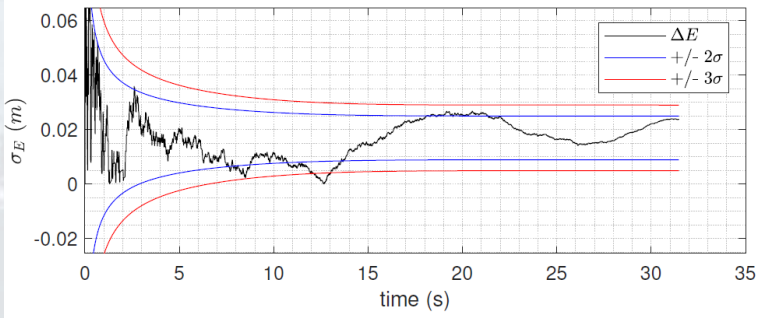
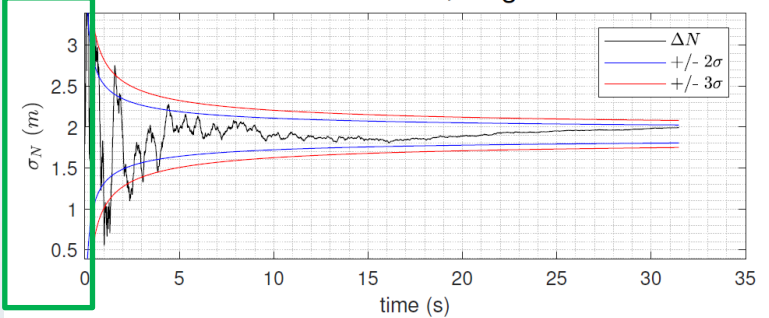
Simulation Results: EKF



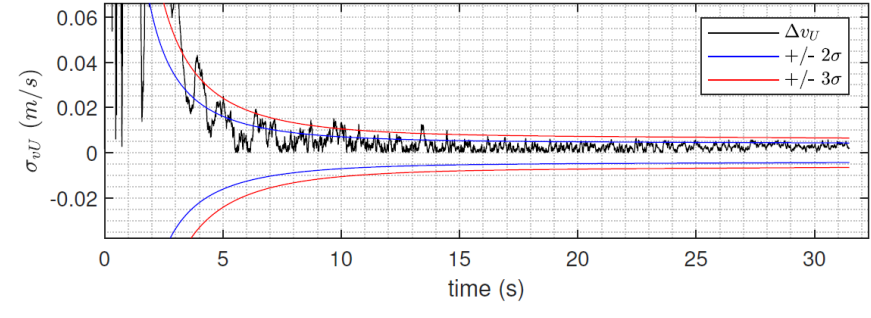
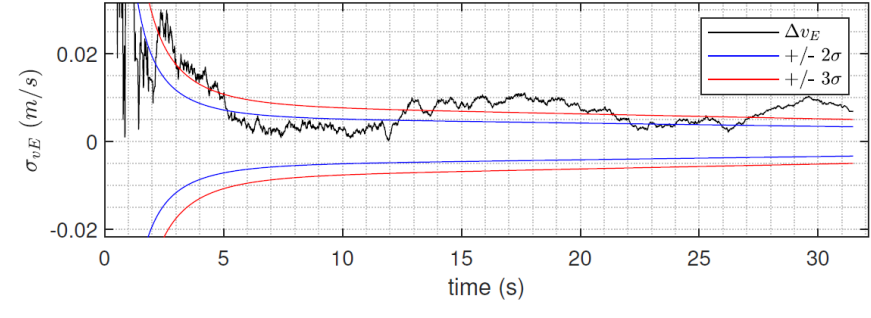
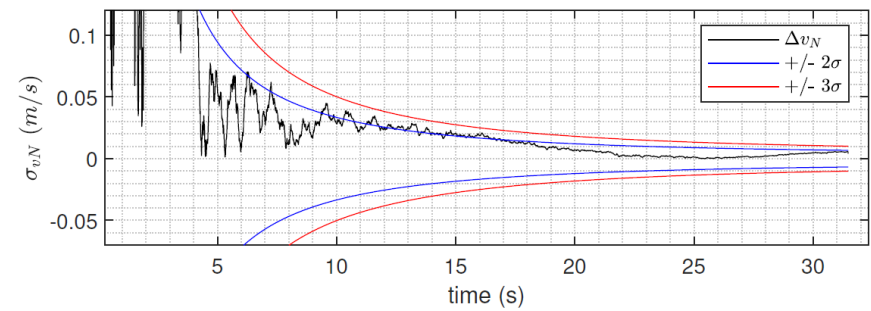
	N	E	U	v_N	v_E	v_U	ϕ	θ	ψ
μ	1.9136	0.01690	0.02258	0.2095	0.02556	0.05556	0.000212	0.000165	0.000467
σ	0.2549	0.009755	0.04175	1.299	0.3620	0.5992	0.000204	0.000114	0.000115

Simulation Results: EKF

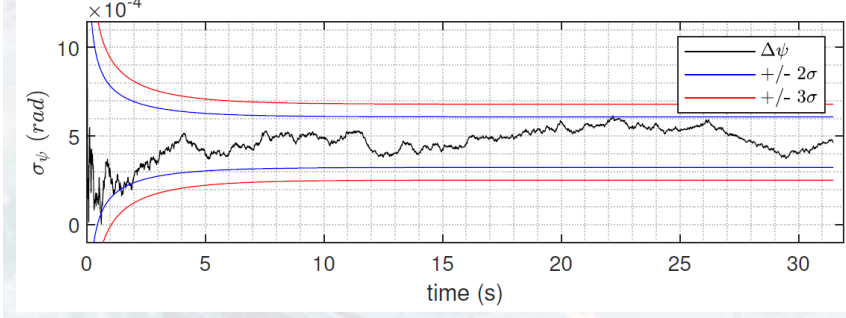
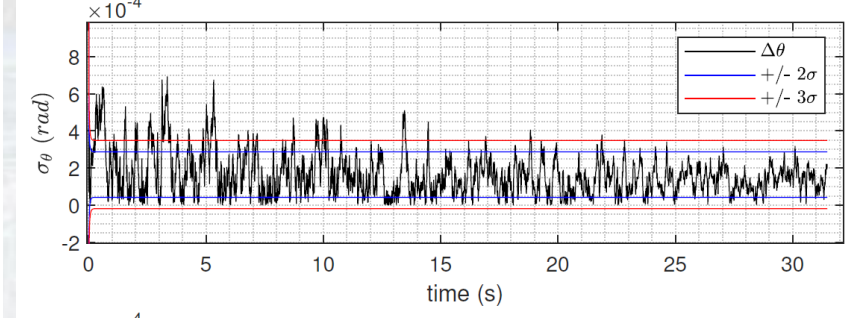
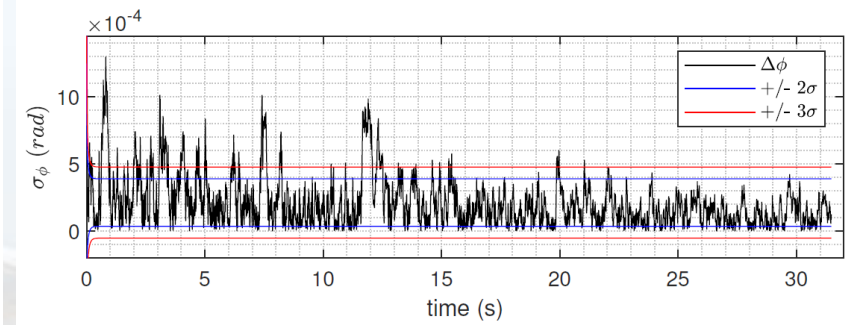
Position error with +/- 2,3 sigma bounds



Velocity Error with +/- 2,3 sigma bounds

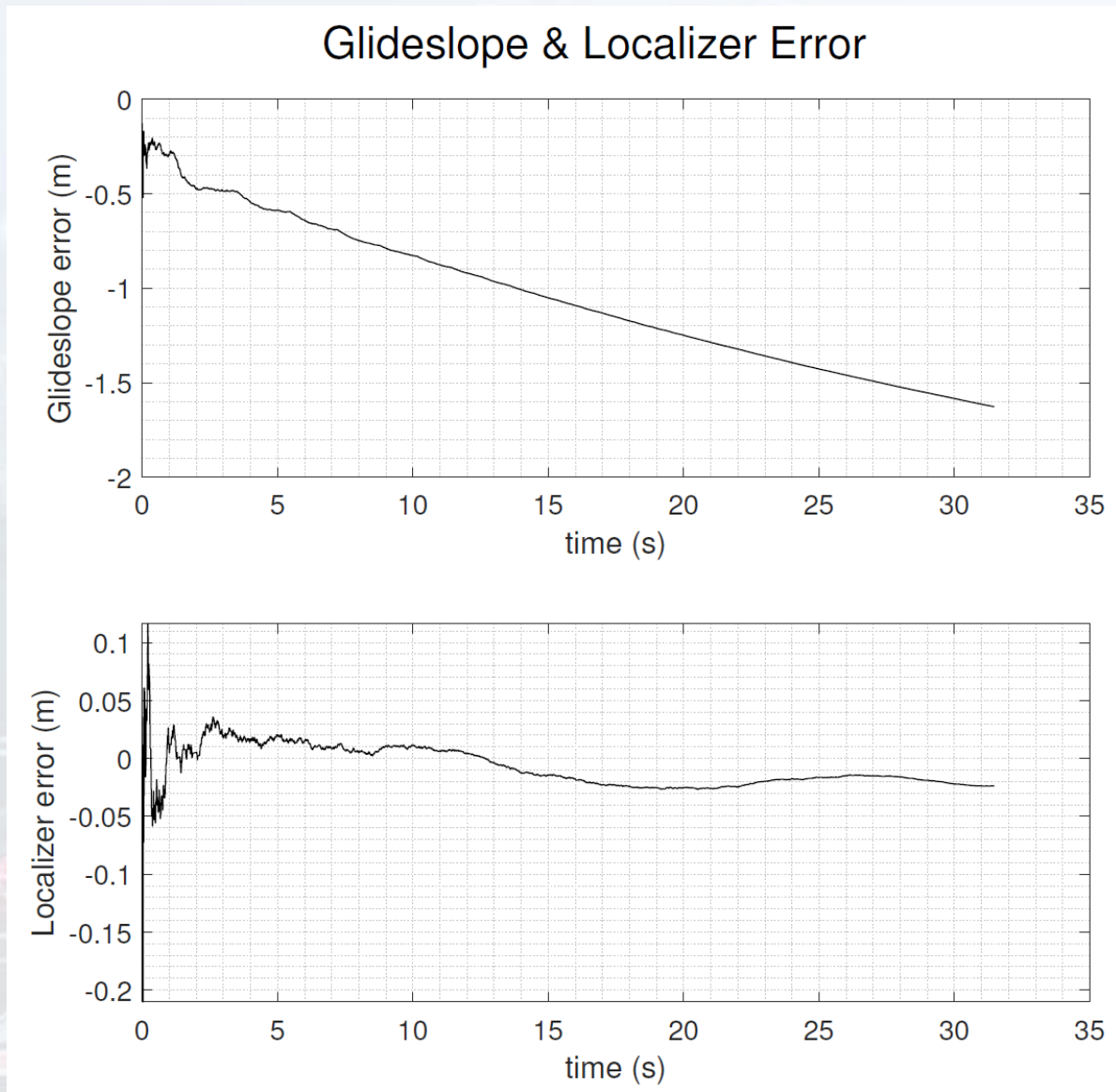


Euler Angle Error with +/- 2,3 sigma bounds



- Errors stay within $\pm 2,3 \sigma$ bounds centered around the mean errors
- Minor fluctuations (small scale)





- Glideslope error diverges due to accumulating minor errors over time
- Localizer error has minor fluctuations due to accurate lateral (East) estimations
- Next step: guidance law based on glideslope and localizer error to return to the nominal glidepath



Simulation Results: X-Plane & World Editor



Outline

1. Introduction
2. Kinematics & Dynamics
3. Tentative Vertiport Landing Light Configuration
4. Approach and Landing Profile
5. Extended Kalman Filter Design
6. Simulation Results
7. Conclusion



Conclusion

- Vision-based navigation solution
- EKF fused VMS IMU telemetry data and coplanar POSIT algorithm (post-processed)
- EKF performance
 - accurate state estimation
 - quick convergence
 - short runtime (2 ms) -> real-time implementation
- Future work
 - Guidance laws for steering aircraft back onto the glidepath based on glideslope & localizer errors
 - Feature correspondence to determine landing lights in pixel coordinates -> high-fidelity X-Plane simulation with coplanar POSIT in real-time



References

1. Federal Aviation Administration, “AC 150/5390-3 (Cancelled) - Vertiport Design,” , 2010. URL https://www.faa.gov/documentLibrary/media/advisory_circular/150-5390-3/150_5390_3.PDF
2. Federal Aviation Administration, “AC 150/5390-2C - Heliport Design,” , 2012. URL https://www.faa.gov/documentLibrary/media/Advisory_Circular/150_5390_2c.pdf
3. National Academies of Sciences, Engineering, and Medicine, *Advancing Aerial Mobility: A National Blueprint*, The National Academies Press, 2020.
4. Wang, Z., Wang, S., Zhu, Y., and Xin, P., “Assessment of ionospheric gradient impacts on ground-based augmentation system (GBAS) data in Guangdong province, China,” *Sensors*, Vol. 17, No. 10, 2017, p. 2313.
5. Oberkampf, D., DeMenthon, D. F., and Davis, L. S., “Iterative pose estimation using coplanar feature points,” *Computer Vision and Image Understanding*, Vol. 63, No. 3, 1996, pp. 495–511.
6. Schaub, H., and Junkins, J. L., *Analytical Mechanics of Space Systems*, 4th ed., AIAA, 2018.
7. Chu, P., Mulder, J. A. B., and Breeman, J., “Real-time identification of aircraft physical models for fault tolerant flight control,” *Fault Tolerant Flight Control*, Springer, 2010, pp. 129–155.
8. Lombaerts, T., Kaneshige, J., Schuet, S., Aponso, B. L., Shish, K. H., and Hardy, G., “Dynamic Inversion based Full Envelope Flight Control for an eVTOL Vehicle using a Unified Framework,” *AIAA Scitech 2020 Forum*, 2020, p. 1619.
9. Webber, D., and Zahn, D., “FAA and the National Campaign,” [Powerpoint], 2021.
10. Stepanyan, V., Lombaerts, T., Shish, K. H., and Cramer, N. B., “Adaptive Multi-Sensor Information Fusion For Autonomous Urban Air Mobility Operations,” *AIAA Scitech 2021 Forum*, 2021, p. 1115.
11. Gelb, A., *Applied Optimal Estimation*, MIT press, 1974.
12. Simon, D., *Optimal State Estimation: Kalman, H1, and Nonlinear Approaches*, John Wiley & Sons, 2006.



Acknowledgements

- Daniel DeMenthon, Computer Scientist – POSIT and SoftPOSIT discussions
- NASA ARC Mentors: Uland Wong & Xavier Bouyssounouse – computer vision & rendering
- NASA ARC Vertical Motion Simulator (VMS) – video and telemetry data
- NASA ARC Data & Reasoning Fabric (DRF) – vertiport locations and trajectory planning



Thank you for listening! Questions?

